

Receiver Operating Characteristic (ROC) Curves

Tilmann Gneiting

Heidelberg Institute for Theoretical Studies, Heidelberg, Germany
Karlsruhe Institute of Technology
tilmann.gneiting@h-its.org

Peter Vogel

Karlsruhe Institute of Technology, Karlsruhe, Germany
Heidelberg Institute for Theoretical Studies
peter.vogel3@kit.edu

September 14, 2018

Abstract

Receiver operating characteristic (ROC) curves are used ubiquitously to evaluate covariates, markers, or features as potential predictors in binary problems. We distinguish raw ROC diagnostics and ROC curves, elucidate the special role of concavity in interpreting and modelling ROC curves, and establish an equivalence between ROC curves and cumulative distribution functions (CDFs). These results support a subtle shift of paradigms in the statistical modelling of ROC curves, which we view as curve fitting. We introduce the flexible two-parameter beta family for fitting CDFs to empirical ROC curves, derive the large sample distribution of the minimum distance estimator and provide software in R for estimation and testing, including both asymptotic and Monte Carlo based inference. In a range of empirical examples the beta family and its three- and four-parameter ramifications that allow for straight edges fit better than the classical binormal model, particularly under the vital constraint of the fitted curve being concave.

1 Introduction

Through all realms of science and society, the assessment of the predictive ability of real-valued markers or features for binary outcomes is of critical importance. To give but a few examples, biomarkers are used to diagnose the presence of cancer or other diseases, numerical weather prediction (NWP) systems serve to anticipate extreme precipitation events, judges need to assess recidivism in convicts, in information retrieval documents, such as websites, are to be classified as signal or noise, banks use customers' particulars to assess credit risk, financial transactions are to be classified as fraud or no fraud, and email messages are to be identified as spam or legitimate. In these and myriads of similar settings, receiver operating characteristic (ROC) curves are key tools in the evaluation of the predictive ability of covariates, markers, or features (Egan et al. 1961, Swets 1973, 1988, Zweig and Campbell 1993, Fawcett 2006). Figure 1 documents the astonishing rise in the use of ROC curves in the scientific literature. In 2017, nearly 8,000 papers were published that use ROC curves, up from less than 50 per year through 1990 and less than 1,000 papers annually through 2002.

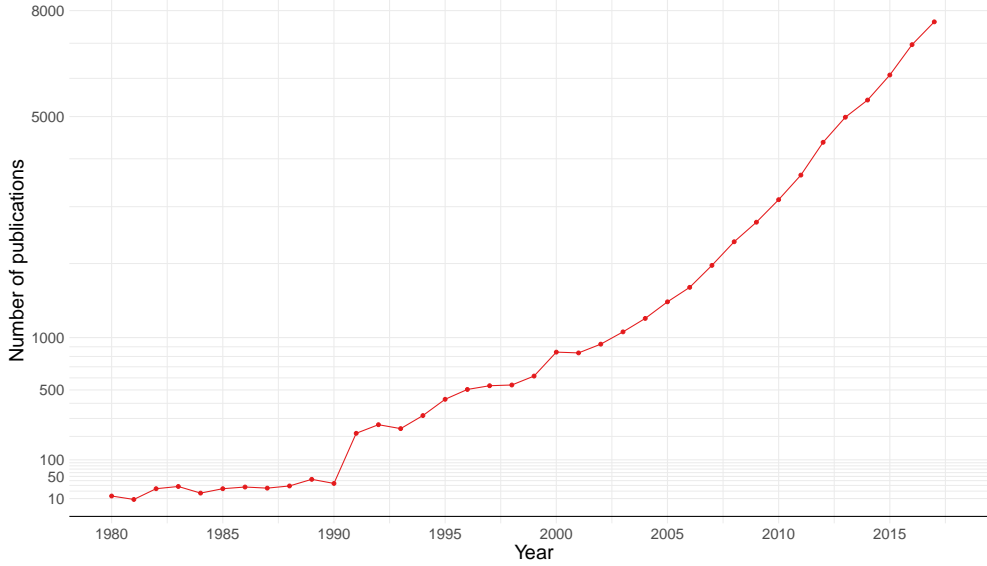


Figure 1: Number of publications per year resulting from a Web of Science topic search for the terms “receiver operating characteristic” or “ROC” on 24 August 2018. Note the square root scale on the vertical axis, which suggests quadratic growth.

A ROC curve is simply a plot of the hit rate (HR) against the false alarm rate (FAR) across the range of thresholds for the real-valued marker or feature at hand. Specifically, consider the joint distribution \mathbb{Q} of the pair (X, Y) , where the covariate, marker or feature X is real-valued, and the event Y is binary, with the implicit understanding that higher values of X provide stronger support for the event to materialize ($Y = 1$). The joint distribution \mathbb{Q} of (X, Y) is characterized by the *prevalence* $\pi_1 = \mathbb{Q}(Y = 1) \in (0, 1)$ along with the conditional cumulative distribution functions (CDFs)

$$F_1(x) = \mathbb{Q}(X \leq x | Y = 1) \quad \text{and} \quad F_0(x) = \mathbb{Q}(X \leq x | Y = 0).$$

Any threshold value x can be used to predict a positive outcome ($Y = 1$) if $X > x$ and a negative outcome ($Y = 0$) if $X \leq x$, to yield a classifier with *hit rate* (HR),¹

$$\text{HR}(x) = \mathbb{Q}(X > x | Y = 1) = 1 - F_1(x),$$

and *false alarm rate* (FAR),

$$\text{FAR}(x) = \mathbb{Q}(X > x | Y = 0) = 1 - F_0(x).$$

¹Terminologies abound and differ markedly between communities. Some researchers talk of ROC as *relative operating characteristic*; see, e.g., Swets (1973) and Mason and Graham (2002). The hit rate has also been referred to as *probability of detection* (POD), *recall*, *sensitivity*, or *true positive rate* (TPR). The false alarm rate is also known as *probability of false detection* (POFD), *fall-out*, or *false positive rate* (FPR) and equals one minus the *specificity*, *selectivity*, or *true negative rate* (TNR). For an overview, see [https://en.wikipedia.org/wiki/Precision_and_recall#Definition_\(classification_context\)](https://en.wikipedia.org/wiki/Precision_and_recall#Definition_(classification_context)), accessed 21 August 2018.

Table 1: Proposed terminology for the potential predictive strength of a feature based on the AUC value.

AUC	Descriptor
> 0.99	nearly perfect
$0.95 - 0.99$	very strong
$0.85 - 0.95$	strong
$0.75 - 0.85$	substantial
$0.65 - 0.75$	moderate
$0.50 - 0.65$	weak
≤ 0.50	abysmal

The term *raw ROC diagnostic* refers to the set-theoretic union of the points of the form $(\text{FAR}(x), \text{HR}(x))'$ within the unit square. The *ROC curve* is a linearly interpolated raw ROC diagnostic, and therefore it also is a point set that may or may not admit a direct interpretation as a function. However, if F_1 and F_0 are continuous and strictly increasing, the raw ROC diagnostic and the ROC curve can be identified with a function R , where $R(0) = 0$,

$$R(p) = 1 - F_1(F_0^{-1}(1 - p)) \quad \text{for } p \in (0, 1), \quad (1)$$

and $R(1) = 1$. High hit rates and low false alarm rates are desirable, so the closer the ROC curve gets to the upper left corner of the unit square the better. The area under the ROC curve (AUC) is a widely used measure of the potential predictive value of a feature (Hanley and McNeil 1982, 1983, DeLong et al. 1988, Bradley 1997), admitting an appealing interpretation as the probability of a marker value drawn from F_1 being higher than a value drawn independently from F_0 . Table 1 proposes terminology for the description of the strength of the potential value in terms of AUC.

In data analytic practice, the measure \mathbb{Q} is the empirical distribution of a sample $(x_i, y_i)_{i=1}^n$ of real-valued features x_i and corresponding binary observations y_i . To generate a ROC curve in this setting, it suffices to consider the unique values of x_1, \dots, x_n and the respective false alarm and hit rates. The resulting raw ROC diagnostic is interpolated linearly to yield an empirical ROC curve, as illustrated in Figure 2 on examples from the biomedical (Etzioni et al. 1999, Sing et al. 2005, Robin et al. 2011) and meteorological (Vogel et al. 2018) literatures. Based on AUC and the terminology in Table 1, the predictor strength is moderate in the example from Robin et al. (2011), substantial for the data from Etzioni et al. (1999) and Vogel et al. (2018), and strong in the example from Sing et al. (2005). Arguably, the immense popularity of empirical ROC curves and AUC across the scientific literature stems from their ease of implementation and interpretation in concert with a wide range of desirable properties, such as invariance under strictly increasing transformations of a feature.

The remainder of the paper is organized as follows. Section 2 establishes some fundamental theoretical results. We formalize the distinction between raw ROC diagnostics and ROC curves, elucidate the special role of concavity in the interpretation and modelling of ROC curves, and demonstrate an equivalence between ROC curves and CDFs.

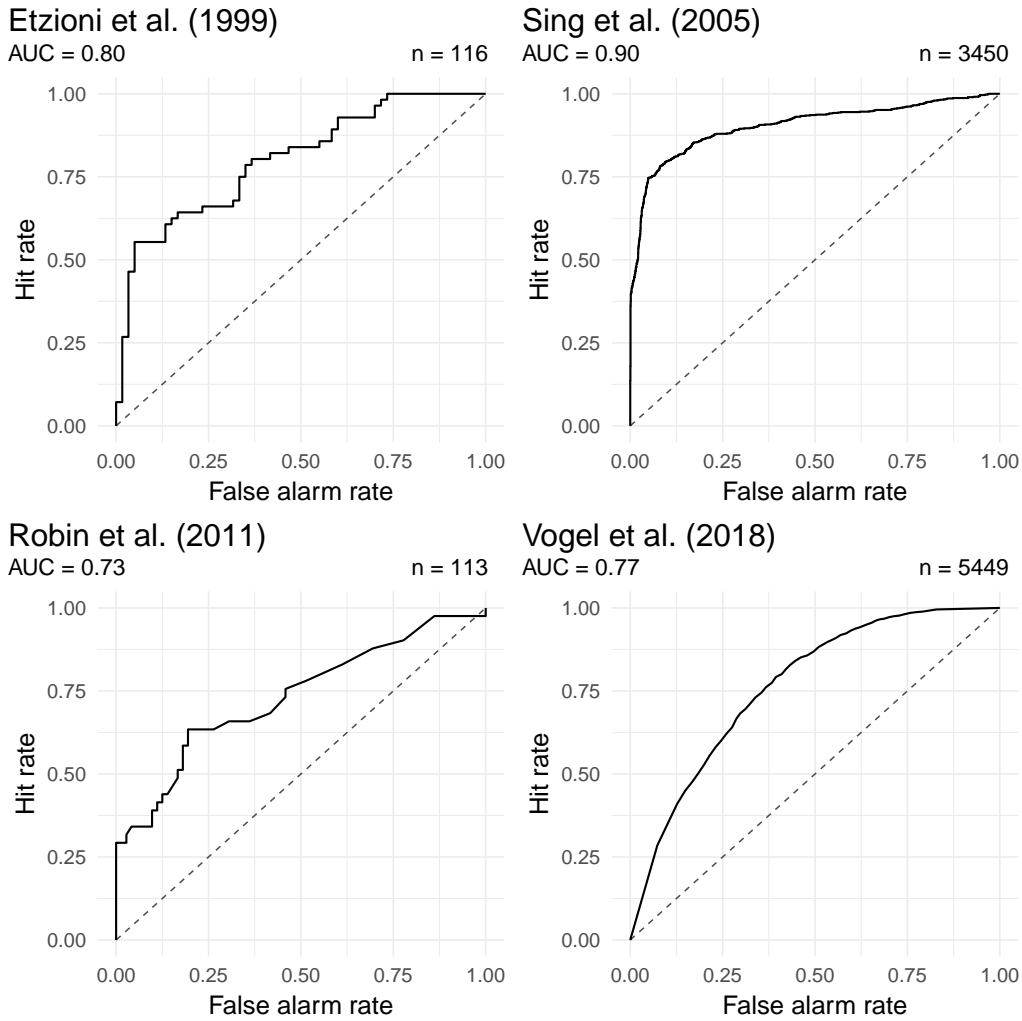


Figure 2: Examples of empirical ROC curves.

In Section 3 we introduce the flexible yet parsimonious two-parameter beta model, which uses the CDFs of beta distributions to model ROC curves, and we discuss estimation and testing based in this context, including both asymptotic and Monte Carlo based approaches. In particular, we derive the large sample distribution of the minimum distance estimator in general parametric settings and specialize to the beta family and the classical binormal model. Section 4 returns to our empirical examples, of which we present detailed analyses, with the beta family and natural three- and four-parameter extensions that allow for straight edges in the ROC curve fitting better than the binormal model, particularly under the constraint of concavity. The paper closes with a discussion in Section 5. Proofs of a more technical character are deferred to Appendix A.

2 Fundamental properties of ROC curves

Consider the bivariate random vector (X, Y) where X is a real-valued predictor, *covariate*, *feature*, or *marker*, and Y is the binary response. We refer to the joint distribution of (X, Y) as \mathbb{Q} . Let $\pi_1 = \mathbb{Q}(Y = 1) \in (0, 1)$ and $\pi_0 = 1 - \pi_1 = \mathbb{Q}(Y = 0)$, and let $F_1(x) = \mathbb{Q}(X \leq x | Y = 1)$, $F_0(x) = \mathbb{Q}(X \leq x | Y = 0)$, and

$$F(x) = \mathbb{Q}(X \leq x) = \pi_0 F_0(x) + \pi_1 F_1(x)$$

denote the conditional and marginal cumulative distribution functions (CDFs) of X , respectively. Furthermore, we let $F_0(x-) = \lim_{x' \uparrow x} F_0(x')$.

We use column vectors to denote points in the Euclidean plane, and given any $(a, b)' \in \mathbb{R}^2$ we write $(a, b)'_{(1)} = a$ and $(a, b)'_{(2)} = b$ for the respective coordinate projections.

2.1 Raw ROC diagnostics and ROC curves

In this common setting ROC diagnostics concern the points of the form $(\text{FAR}(x), \text{HR}(x))'$, where $\text{FAR}(x) = 1 - F_0(x)$ is the *false alarm rate* and $\text{HR}(x) = 1 - F_1(x)$ the *hit rate* at the threshold value $x \in \mathbb{R}$. Formally, the *raw ROC diagnostic* for the random vector (X, Y) and the bivariate distribution \mathbb{Q} is the point set

$$R^* = \left\{ \begin{pmatrix} 1 - F_0(x) \\ 1 - F_1(x) \end{pmatrix} : x \in \mathbb{R} \right\} \quad (2)$$

within the unit square. Clearly, the bivariate distribution \mathbb{Q} of (X, Y) is characterized by F_0 , F_1 , and any of the two marginal distributions. In contrast, the raw ROC diagnostic along with a single marginal does not characterize \mathbb{Q} , due to the well known invariance of ROC diagnostics under strictly increasing transformations of X and shifts in the prevalence of the binary outcome (Fawcett 2006). However, the raw ROC diagnostic along with both marginal distributions determines \mathbb{Q} .

Theorem 1. *The joint distribution \mathbb{Q} of (X, Y) is characterized by the raw ROC diagnostic and the marginal distributions of X and Y .*

Proof. The mapping $g : [0, 1]^2 \rightarrow [0, 1]$ defined by

$$(a, b)' \mapsto (1 - a)\pi_0 + (1 - b)\pi_1$$

induces a bijection between the raw ROC diagnostic R^* and the range of F . Therefore, it suffices to note that $\mathbb{Q}(X \leq x, Y \leq y) = 0$ for $y < 0$,

$$\begin{aligned} \mathbb{Q}(X \leq x, Y \leq y) &= F_0(x) \pi_0 \\ &= F(x) - (1 - \text{HR}(x)) \pi_1 \\ &= F(x) - (1 - g_{(2)}^{-1}(F(x))) \pi_1 \end{aligned}$$

for $y \in [0, 1)$, and $\mathbb{Q}(X \leq x, Y \leq y) = F(x)$ for $y \geq 1$. \square

Table 2: Ordered marker values $x_1 < x_2 < \dots < x_7$, binary observations, and false alarm rate (FAR) and hit rate (HR) at the respective threshold for the example in Figure 3.

X	$< x_1$	x_1	x_2	x_3	x_4	x_5	x_6	x_7	$> x_7$
Y		0	1	0, 0	0, 0, 1	0, 1, 1	1	1	
FAR $\times 6$	6	5	5	3	1	0	0	0	0
HR $\times 6$	6	6	5	5	4	2	1	0	0

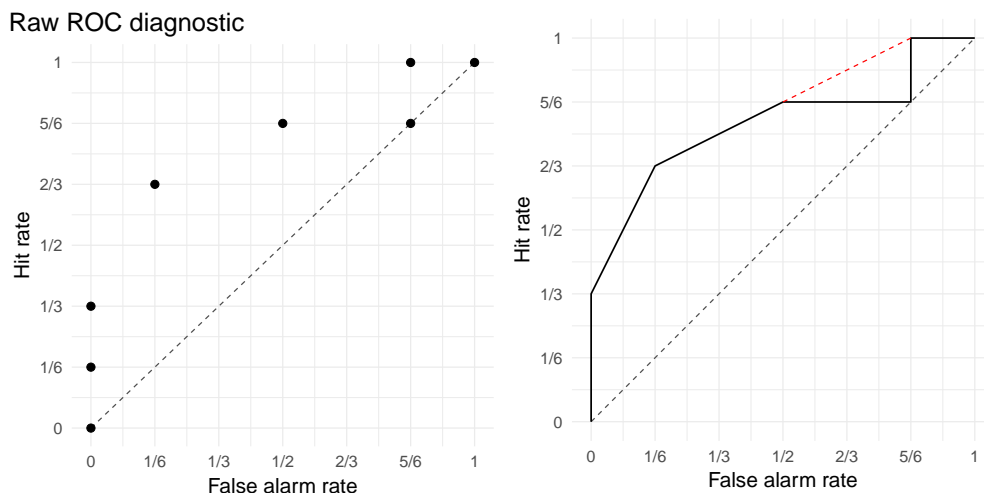


Figure 3: Raw ROC diagnostic and corresponding empirical ROC curve for the marker in Table 2. The broken red line completes the concave hull of the empirical ROC curve.

Briefly, a ROC curve is obtained from the raw ROC diagnostic by linear interpolation. Formally, the *full ROC diagnostic* or *ROC curve* is the point set

$$R = \left\{ \begin{pmatrix} 0 \\ 0 \end{pmatrix} \right\} \cup R^* \cup \{L_x : x \in \mathbb{R}\} \cup \left\{ \begin{pmatrix} 1 \\ 1 \end{pmatrix} \right\} \quad (3)$$

within the unit square, where

$$L_x = \left\{ \alpha \begin{pmatrix} 1 - F_0(x^-) \\ 1 - F_1(x^-) \end{pmatrix} + (1 - \alpha) \begin{pmatrix} 1 - F_0(x) \\ 1 - F_1(x) \end{pmatrix} : \alpha \in [0, 1] \right\}$$

is a possibly degenerate, nondecreasing line segment. The choice of linear interpolation to complete the raw ROC diagnostic into the ROC curve (3) is natural and persuasive, as the line segment L_x represents randomized combinations of the classifiers associated with its end points. In particular, linear interpolation allows for a fair and direct comparison between continuous, discrete, and ordinal features. Empirical ROC curves based on samples, as illustrated in Figure 2, fit this framework, as they arise in the special case where \mathbb{Q} is an empirical measure. We illustrate the transition from the raw ROC

diagnostic to the ROC curve in Figure 3 using the toy data set from Table 2, where there are twelve observations and seven unique marker values.

The raw ROC diagnostic can be recovered from the ROC curve and the two marginal distributions, as the mapping g in the proof of Theorem 1 induces a bijection between the raw ROC diagnostic and the range of F that can be expressed in terms of π_1 and π_0 . From this simple fact the following result is immediate.

Corollary 2. *The joint distribution \mathbb{Q} of (X, Y) is characterized by the ROC curve and the marginal distributions of X and Y .*

In this sense, ROC curves and raw ROC diagnostics assume roles similar to those of copulas (e.g., Nelsen 2006), with the difference that ROC characteristics are defined in terms of conditional distributions, whereas copulas operate on marginal distributions.

Given a ROC curve R , an obvious task is to find CDFs F_0 and F_1 that realize R . For a particularly simple and appealing construction, let F_0 be the CDF of the uniform distribution on the unit interval, and take F_1 to be F_{NI} , defined as $F_{\text{NI}}(x) = 0$ for $x \leq 0$,

$$F_{\text{NI}}(x) = 1 - R_+(1 - x) \quad \text{for } x \in (0, 1), \quad (4)$$

and $F_{\text{NI}}(x) = 1$ for $x \geq 1$, where the function $R_+ : (0, 1) \rightarrow [0, 1]$ is induced by the ROC curve at hand, in that

$$R_+(x) = \inf \{b : (a, b)' \in R, a \geq x\}.$$

In anticipation of its repeated use in subsequent sections, we refer to this specific realization of a ROC curve R , in which F_0 is standard uniform and F_1 is taken to be F_{NI} in (4), as the *natural identification*.

Remarkably, the natural identification applies even when the feature X is discrete or ordinal. Nevertheless, the statistical models and methods that we introduce in Section 3 target the case of a continuous marker or feature.

2.2 Concave ROC curves

We proceed to elucidate the critical role of concavity in the interpretation and modelling of ROC curves.² Its significance is well known and has been alluded to in monographs, such as in Egan (1975, p. 35), Pepe (2003, p. 71), and Zhou et al. (2011, p. 40). Nevertheless, we are unaware of any rigorous treatment in the extant literature. To address this omission, we distinguish and analyse regular and discrete settings. Unified treatments are feasible but considerably technical, and we leave them to future work.

In the *regular setting* we suppose that F_1 and F_0 have continuous, strictly positive Lebesgue densities f_1 and f_0 in the interior of an interval, which is their common support.

²Again, terminologies differ between communities. In machine learning, concave ROC curves are typically referred to as *convex* (e.g., Fawcett 2006), whereas the psychological and biomedical literatures call them *proper* (Egan 1975, Section 2.6, Zhou et al. 2011, Section 2.7.3). The usage in this paper is in accordance with well established, commonly used terminology in the mathematical sciences.

For every x in the interior of the support, we can define the *likelihood ratio*,

$$\text{LR}(x) = \frac{f_1(x)}{f_0(x)},$$

and the *conditional event probability*,

$$\text{CEP}(x) = \mathbb{Q}(Y = 1 | X = x) = \frac{\pi_1 f_1(x)}{\pi_0 f_0(x) + \pi_1 f_1(x)}.$$

We demonstrate the equivalence of the following three conditions:

- (a) The ROC curve is concave.
- (b) The likelihood ratio is nondecreasing.
- (c) The conditional event probability is nondecreasing.

Theorem 3. *In the regular setting statements (a), (b), and (c) are equivalent.*

Proof. In the regular setting the ROC curve can be identified with a function $R : [0, 1] \rightarrow [0, 1]$, where $R(p)$ is defined as in (1) for $p \in (0, 1)$. If the ROC curve is concave then clearly the function R is concave as well, and so its derivative $R'(p)$ is nonincreasing in $p \in (0, 1)$. However, the slope $R'(p)$ equals the likelihood ratio $\text{LR}(x)$ at a certain value x that decreases with p , which establishes the equivalence of (a) and (b). Furthermore,

$$\text{LR}(x) = \frac{\pi_0}{\pi_1} \frac{\text{CEP}(x)}{1 - \text{CEP}(x)},$$

and the function $c \mapsto c/(1-c)$ is nondecreasing in $c \in (0, 1)$, which yields the equivalence of (b) and (c). \square

Next we consider the *discrete setting* in which the support of the feature X is a finite or countably infinite set. This setting includes, but is not limited to, the case of empirical ROC curves, as illustrated in Figure 2. For every x in the discrete support of X , we can define the *likelihood ratio*,

$$\text{LR}(x) = \begin{cases} \mathbb{Q}(X = x | Y = 1) / \mathbb{Q}(X = x | Y = 0) & \text{if } \mathbb{Q}(X = x | Y = 0) > 0, \\ \infty, & \text{if } \mathbb{Q}(X = x | Y = 0) = 0, \end{cases}$$

and the *conditional event probability*,

$$\text{CEP}(x) = \mathbb{Q}(Y = 1 | X = x).$$

In Appendix A.1 we prove the following direct analogue of Theorem 3.

Theorem 4. *In the discrete setting statements (a), (b), and (c) are equivalent.*

The critical role of concavity in the interpretation and modelling of ROC curves stems from the monotonicity condition (c) on the conditional event probability, which is at the very heart of the approach and needs to be invoked to justify the construction of just any raw ROC diagnostic or ROC curve. In the medical literature Hilden (1991) notes that “some authors do seem to overlook the concavity problem” and Pesce et al. (2010) argue that “direct use of a decision variable” with a non-concave ROC curve “must be considered irrational” and “unethical when applied to medical decisions”. Similar considerations apply in the vast majority of applications of ROC curves.

Fortunately, there are straightforward ways of restricting attention to concave ROC curves and the associated classifiers. Generally, randomization can be used to generate classifiers with concave ROC curves from features with non-concave ones (Fawcett 2006, Pesce et al. 2010). The regular setting serves to supply theoretical models that can be fit to empirical ROC curves, such as the classical binormal model or our new beta model, and the parameters in these models can be restricted suitably to guarantee concavity, as we discuss in Section 3. Empirical ROC curves typically fail to be concave, as illustrated in Figure 2. However, they can readily be morphed into their concave hull, by subjecting the marker or feature at hand to the pool-adjacent violators (PAV: Ayer et al. 1955, de Leeuw et al. 2009) algorithm, thereby converting it into an isotonic, calibrated probabilistic classifier (Lloyd 2002, Fawcett and Niculescu-Mizil 2007). For example, for the toy data in Table 3 the PAV algorithm assigns the conditional event probability $p_1 = 0$ to x_1 , the value $p_2 = \frac{1}{3}$ to x_2, x_3 , and x_4 , the value $p_3 = \frac{2}{3}$ to x_5 , and the value $p_4 = 1$ to x_6 and x_7 . The ROC curve for this isotonic and calibrated probabilistic classifier is the concave hull of the ROC curve for the original marker, as shown in Figure 3.

2.3 An equivalence between ROC curves and probability measures

We move on to provide concise and practically relevant characterizations of ROC curves, both with and without the critical condition of concavity.

Theorem 5. *There is a one-to-one correspondence between ROC curves and probability measures on the unit interval. In particular, the natural identification induces a bijection between the class of the ROC curves and the class of the CDFs of probability measures on the unit interval.*

Proof. Given a ROC curve, we remove any vertical line segments, except for the respective upper endpoints, to yield the CDF of a probability measure on the unit interval. Conversely, given the CDF of a probability measure on the unit interval, we interpolate vertically at any jump points to obtain a ROC curve. This mapping is a bijection, and save for the symmetries in (4) it is realized by the natural identification. \square

We say that a curve C in the Euclidean plane is nondecreasing if $a_0 \leq a_1$ is equivalent to $b_0 \leq b_1$ for points $(a_0, b_0)', (a_1, b_1)' \in C$. The following result is immediate.

Corollary 6. *The ROC curves are the nondecreasing curves in the unit square that connect the points $(0, 0)'$ and $(1, 1)'$.*

We now state characterizations under the constraint of strict concavity. Analogous results hold under the slightly weaker assumption of concavity.

Theorem 7. *There is a one-to-one correspondence between strictly concave ROC curves and probability measures with strictly decreasing Lebesgue densities on the unit interval, which is induced by the natural identification.*

Corollary 8. *The strictly concave ROC curves are in one-to-one correspondence to the strictly concave functions R on the unit interval with $R(0) = 0$ and $R(1) = 1$.*

Turning to methodological and applied considerations, these results support a shift of paradigms in the statistical modelling of ROC curves. In extant practice, the emphasis is on modelling the conditional distributions F_0 and F_1 , such as in the ubiquitous binormal model. Our results suggest a subtle but important change of perspective, in that ROC modelling can be approached as an exercise in curve fitting,³ with any nondecreasing curve that connects $(0, 0)'$ to $(1, 1)'$ being a permissible candidate, and parametric families of CDFs on the unit interval offering particularly attractive models, including but not limited to the beta family that we introduce in the next section.

3 Parametric models, estimation, and testing

The binormal model is by far the most frequently used parametric model and “plays a central role in ROC analysis” (Pepe 2003, p. 81). Specifically, the binormal model assumes that F_1 and F_0 are Gaussian with means $\mu_1 \geq \mu_0$ and strictly positive variances σ_0^2 and σ_1^2 , respectively. We are in the regular setting of Section 2.2, and the resulting ROC curve is represented by the function $R : [0, 1] \rightarrow [0, 1]$ with $R(0) = 0$,

$$R(p) = \Phi(\mu + \sigma\Phi^{-1}(p)) \quad \text{for } p \in (0, 1), \quad (5)$$

and $R(1) = 1$, where Φ is the CDF of the standard normal distribution, $\mu = (\mu_1 - \mu_0)/\sigma_1 \geq 0$ is a scaled difference in expectations, and $\sigma = \sigma_0/\sigma_1$ is the ratio of the respective standard deviations. The respective area under the curve is

$$\text{AUC}(\mu, \sigma) = \Phi\left(\frac{\mu}{\sqrt{1 + \sigma^2}}\right).$$

For an illustration of binormal ROC curves see the left-hand panel of Figure 4. It is well known that a binormal ROC curve is concave only if $\sigma = 1$ or equivalently if F_0 and F_1 differ in location only. These curves are necessarily symmetric with respect to the anti-diagonal in the unit square, thereby strongly inhibiting their flexibility, as illustrated in the left-hand panel of Figure 5.

³While curve fitting approaches have been advocated before, such as by Swets (1986, p. 104, his approach (b)), they lacked theoretical support.

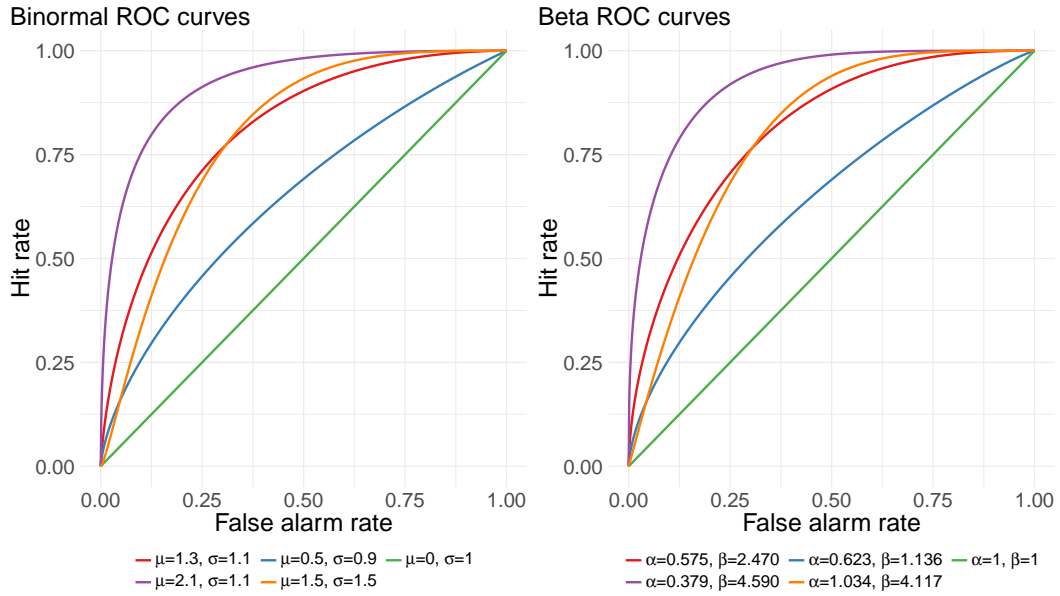


Figure 4: Members of the (left) binormal family and (right) beta family of ROC curves. The parameter values for the beta curves have been chosen to match the overall shape of the same-color binormal ROC curve.

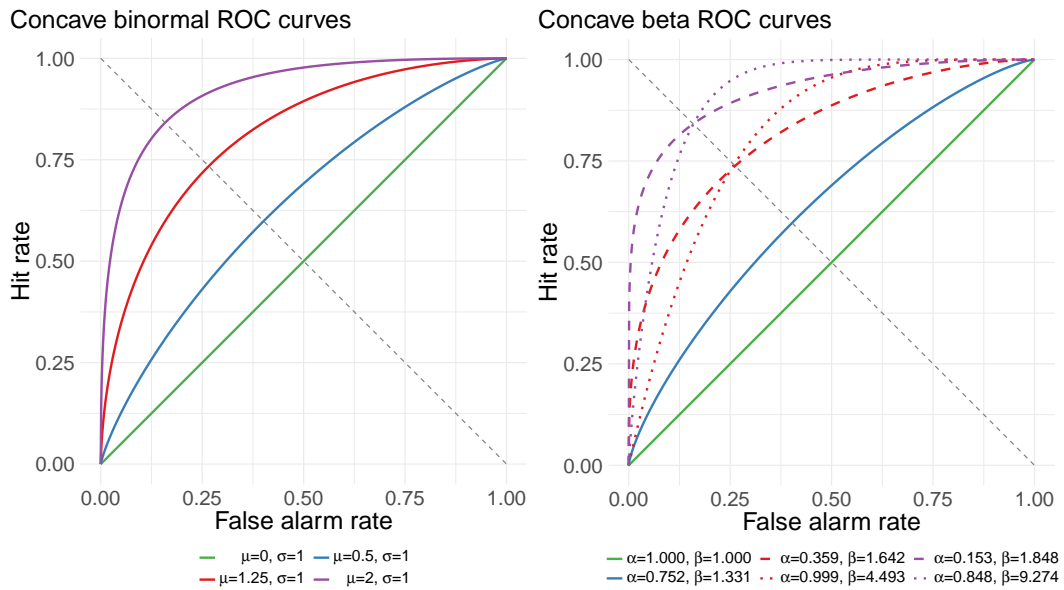


Figure 5: Concave members of the (left) binormal family and (right) beta family of ROC curves. The parameter values for the beta curves have been chosen to match the value of the same-color binormal ROC curve at the anti-diagonal.

3.1 The beta model

Motivated and supported by the characterization theorems of Section 2, we propose a curve fitting approach to the statistical modelling of ROC curves, with the two-parameter family of the cumulative distribution functions (CDFs) of beta distributions being a particularly attractive model. Specifically, consider the beta family with ROC curves represented by the function

$$R(p) = B_{\alpha,\beta}(p) = \int_0^p b_{\alpha,\beta}(q) dq \quad \text{for } p \in [0, 1], \quad (6)$$

where $b_{\alpha,\beta}(q) \propto q^{\alpha-1}(1-q)^{\beta-1}$ is the density of the beta distribution with parameter values $\alpha > 0$ and $\beta > 0$. As illustrated in Figure 6 and shown in Appendix A.2, a beta ROC curve is concave if $\alpha \leq 1$ and $\beta \geq 2 - \alpha$, and its AUC value is

$$\text{AUC}(\alpha, \beta) = \frac{\beta}{\alpha + \beta}.$$

In the limit as $\beta \rightarrow \infty$ we obtain the perfect ROC curve with straight edges from $(0, 0)'$ to $(0, 1)'$ and $(1, 1)'$, corresponding to a complete separation of the supports of F_1 and F_0 . While the requirement of a concave ROC curve is restrictive, the condition is much less stringent than for the binormal family, where it constrains the admissible parameter space to a single dimension. The adaptability of the beta family is illustrated in Figure 4, where we see that members of the beta family can match the shape of binormal ROC curves, and in Figure 5, where the gain in flexibility under the critical constraint of concavity is evident.

The beta family nests the time-honored one-parameter power model (Egan et al. 1961, Swets 1986) that arises in the special case when $\beta = 1$. While the classical derivation of the power model does not readily generalize, our theoretical results justify the use of the two-parameter beta family. If even further flexibility is desired, mixtures of beta CDFs, i.e., functions of the form

$$R_n(p) = \sum_{k=1}^n w_k B_{\alpha_k, \beta_k}(p) \quad \text{for } p \in [0, 1],$$

where $w_1, \dots, w_n \geq 0$ with $w_1 + \dots + w_n = 1$, $\alpha_1, \dots, \alpha_k > 0$, and $\beta_1, \dots, \beta_k > 0$, approximate any regular ROC curve to any desired accuracy, as demonstrated by the following result. Recall from Section 2.2 that in the regular setting the ROC curve can be identified with the function R in (1), where F_1 and F_0 have continuous, strictly positive Lebesgue densities f_1 and f_0 in the interior of an interval, which is their common support. A ROC curve is *regular* if it arises in this way and *strongly regular* if furthermore the derivative R' is bounded.

Theorem 9. *For every strongly regular ROC curve R there is a sequence of mixtures of beta CDFs that converges uniformly to R .*

The proof of this result relies on Bernstein's probabilistic approach to the Weierstrass theorem (Levasseur 1984) and is deferred to Appendix A.2.

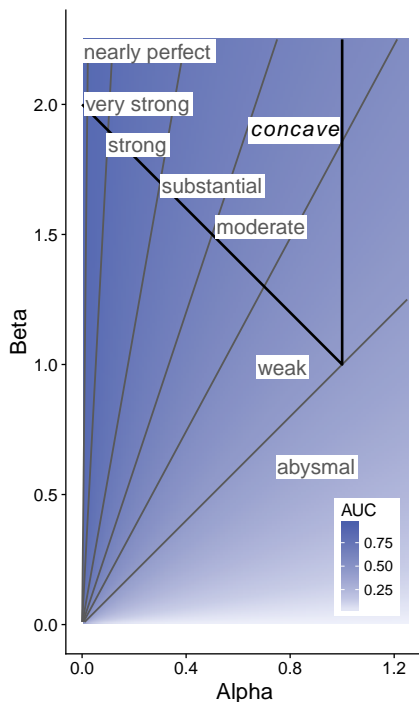


Figure 6: AUC value for the beta family of ROC curves. The isolines correspond to the terminology for predictor strength introduced in Table 1. Parameter combinations above the thick line yield concave ROC curves.

3.2 Minimum distance estimation

For the parametric estimation of ROC curves for continuous markers various methods have been proposed, including maximum likelihood (Dorfman and Alf 1969, Metz et al. 1998, Zou and Hall 2000), approaches based on generalized linear models (Pepe 2000), and minimum distance estimation (Hsieh and Turnbull 1996), as reviewed at book length by Pepe (2003), Krzanowski and Hand (2009), and Zhou et al. (2011). Maximum likelihood techniques face a conceptual challenge, in that ROC curves do not determine the joint distribution of the marker and the binary event. Here we pursue the minimum distance estimator, which is much in line with our curve fitting approach.

We assume a parametric model in the regular setting of Section 2.2, where now the ROC curve depends on a parameter $\theta \in \Theta \subseteq \mathbb{R}^k$. Specifically, we suppose that for each $\theta \in \Theta$ the ROC curve is represented by a smooth function

$$R(p; \theta) = 1 - F_{1,\theta}(F_{0,\theta}^{-1}(1 - p)) \quad \text{for } p \in (0, 1),$$

where $F_{1,\theta}$ and $F_{0,\theta}$ admit continuous, strictly positive densities $f_{1,\theta}$ and $f_{0,\theta}$ in the interior of an interval, which is their common support. We also require that the true

parameter value θ_0 is in the interior of the parameter space Θ , where the derivative

$$R'(p; \theta) = \frac{\partial R(p; \theta)}{\partial p} = \frac{f_{1,\theta}(F_{0,\theta}^{-1}(1-p))}{f_{0,\theta}(F_{0,\theta}^{-1}(1-p))}$$

exists and is finite for $p \in (0, 1)$, and where the partial derivative $R_{(i)}(p; \theta)$ of $R(p; \theta)$ with respect to component i of the parameter vector $\theta = (\theta_1, \dots, \theta_k)'$ exists and is continuous for $i = 1, \dots, k$ and $p \in (0, 1)$.

We adopt the asymptotic scenario of Hsieh and Turnbull (1996), where at sample size n there are n_0 and $n_1 = n - n_0$ independent draws from $F_{0,\theta}$ and $F_{1,\theta}$ with corresponding binary outcomes of zero and one, respectively, where $\lambda_n = n_0/n_1$ converges to some $\lambda \in (0, 1)$ as $n \rightarrow \infty$. For $\theta \in \Theta$ we define the difference process

$$\xi_n(p; \theta) = \hat{R}_n(p) - R(p; \theta),$$

where the function $\hat{R}_n(p)$ represents the empirical ROC curve. The minimum distance estimator $\hat{\theta}_n = (\hat{\theta}_1, \dots, \hat{\theta}_k)'$ then satisfies

$$\|\xi_n(\cdot; \hat{\theta}_n)\| = \min_{\theta \in \Theta} \|\xi_n(\cdot; \theta)\|,$$

where $\|\xi_n(\cdot; \theta)\| = (\int_0^1 \xi_n(p; \theta)^2 dp)^{1/2}$ is the standard L_2 -norm. If n is large, $\hat{\theta}_n$ exists and is unique with probability approaching one (Millar 1984), and so we follow the extant literature in ignoring issues of existence and uniqueness.

The minimum distance estimator has a multivariate normal limit distribution in this setting, as suggested by the asymptotic result of Hsieh and Turnbull (1996) that under the usual \sqrt{n} scaling the difference process $\xi_n(p; \theta)$ has limit

$$W(p; \theta) = \sqrt{\lambda} B_1(R(p; \theta)) + R'(p; \theta) B_2(p) \quad (7)$$

at $\theta = \theta_0$, where B_1 and B_2 are independent copies of a Brownian bridge. In Appendix A.3 we review the specifics of the convergence to the limit process (7) and combine results of Millar (1984) and Hsieh and Turnbull (1996) to show the following result.

Theorem 10. *In the above setting the minimum distance estimator $\hat{\theta}_n$ satisfies*

$$\sqrt{n}(\hat{\theta}_n - \theta_0) \rightarrow \mathcal{N}(0, C^{-1}AC^{-1}) \quad (8)$$

as $n \rightarrow \infty$, where the matrices A and C have entries

$$A_{ij} = \int_0^1 \int_0^1 R_{(i)}(s; \theta_0) K(s, t; \theta_0) R_{(j)}(t; \theta_0) ds dt, \quad C_{ij} = \int_0^1 R_{(i)}(s; \theta_0) R_{(j)}(s; \theta_0) ds \quad (9)$$

for $i, j = 1, \dots, k$, respectively, and where

$$K(s, t; \theta_0) = \lambda(\min\{R(s; \theta_0), R(t; \theta_0)\} - R(s; \theta_0)R(t; \theta_0)) + R'(s; \theta_0)R'(t; \theta_0)(\min\{s, t\} - st). \quad (10)$$

is the covariance function of the process $W(p; \theta)$ in (7) at $\theta = \theta_0$.

Corollary 11. *In the above setting,*

$$\sqrt{n}(\text{AUC}(\hat{\theta}_n) - \text{AUC}(\theta_0)) \rightarrow \mathcal{N}(0, GC^{-1}AC^{-1}G'), \quad (11)$$

where G is the gradient of the mapping $\theta \mapsto \text{AUC}(\theta)$ at $\theta = \theta_0$.

Both the binormal and the beta model satisfy the assumptions for these results, which allow for asymptotic inference about the model parameters and the AUC, by plugging in $\hat{\theta}_n$ for θ_0 in the expressions for the asymptotic covariances. For the binormal model (5) we have $\theta = (\mu, \sigma)$, $R_{(\mu)}(p; \theta) = \varphi(\mu + \sigma\Phi^{-1}(p))$, $R_{(\sigma)}(p; \theta) = \Phi^{-1}(p)\varphi(\mu + \sigma\Phi^{-1}(p))$, and $R'(p; \theta) = \sigma\varphi(\mu + \sigma\Phi^{-1}(p))/\varphi(\Phi^{-1}(p))$, where φ is the standard normal density, so that the integrals in (9) can readily be evaluated numerically. The gradient in (11) equals $G = (\varphi(\mu_0/\sqrt{1 + \sigma_0^2})/(1 + \sigma_0^2)^{1/2}, -\mu_0\sigma_0\varphi(\mu_0/\sqrt{1 + \sigma_0^2})/(1 + \sigma_0^2)^{3/2})$. Hsieh and Turnbull (1996) consider binormal ordinal dominance curves, which interchange the roles of F_1 and F_0 relative to ROC curves, and after reparameterization we recover their results. However, the formula for the covariance function $K(s, t; \theta)$ in the first displayed equation on page 39 in Hsieh and Turnbull (1996) is incompatible with our equation (10) and incorrect, as it is independent of s and t and therefore constant. Under the beta model (6) we have $\theta = (\alpha, \beta)$ and $R'(p; \theta) = b_{\alpha, \beta}(p)$. While closed form expressions for the partial derivatives of $R(p; \theta)$ with respect to α and β exist, they are difficult to evaluate, and we approximate them with finite differences. The gradient in (11) equals $G = (-\beta_0/(\alpha_0 + \beta_0)^2, \alpha_0/(\alpha_0 + \beta_0)^2)$.

3.3 Testing goodness-of-fit and other hypotheses

We move on to discuss testing. A natural hypothesis to be addressed is whether a given parametric model fits the data at hand. In contrast to existing methods that are based on AUC and focus on the binormal model (Zou et al. 2005), we propose a simple Monte Carlo test that applies to any parametric model \mathcal{C} . For example, \mathcal{C} could be the full binormal, the concave binormal, the full beta, or the concave beta family. While we describe the procedure for minimum distance estimates and the L_2 -distance, it applies equally to other estimates and other distance measures.

Given a dataset of size n with n_0 instances where the binary outcome is zero and $n_1 = n - n_0$ instances where it is one, our goodness-of-fit test proceeds as follows. We use the notation of Section 3.2 and denote the number of Monte Carlo replicates by M .

1. Fit a model from class \mathcal{C} to the empirical ROC curve for the data at hand, to yield the minimum distance estimate θ_{data} . Compute d_{data} as the L_2 -distance between the fitted and the empirical ROC curve.
2. For $m = 1, \dots, M$,
 - (a) draw a sample of size n under θ_{data} , with n_0 and n_1 instances from $F_{0, \theta_{\text{data}}}$ and $F_{1, \theta_{\text{data}}}$ and associated binary outcomes of zero and one, respectively,
 - (b) fit a model from class \mathcal{C} to the empirical ROC curve, to yield the minimum distance estimate, and

- (c) compute d_m as the L_2 -distance between the fitted and the empirical ROC curve.
3. Find a p -value based on the rank of d_{data} when pooled with d_1, \dots, d_M . Specifically, $p = (\#\{i = 1, \dots, M : d_{\text{data}} \leq d_i\} + 1)/(M + 1)$.

Under the null hypothesis of the ROC curve being generated by a random sample within class \mathcal{C} the Monte Carlo p -value is very nearly uniformly distributed, as is readily seen in simulation experiments (not reported on here).

Parametric tests of the equality of ROC curves and AUC values can be based on the limit distributions in Theorem 10 and Corollary 11 in the usual way. Under an identifiable model the hypothesis of two ROC curves being equal is the same as the hypothesis of the respective parameters being the same. Therefore, the limit in (8) allows for a customary chi square test of the equality of ROC curves from independent samples, based on the squared norm of the normalized difference between the two estimates of the parameter vector, as proposed by Metz and Kronman (1980) in the case of maximum likelihood estimates under the binormal model. Similarly, the limit in (11) justifies a z -test for the equality of the AUC values, based on the normalized difference between the two parametric estimates of the AUC. We illustrate the use of these tests in the subsequent section and provide software for their implementation in the case of independent samples. For paired, dependent samples, correlations between the estimates need to be accounted for, a task to be addressed in future work. As an alternative, nonparametric tests have been developed in the extant literature (Hanley and McNeil 1983, DeLong et al. 1988, Venkatraman and Begg 1996, Venkatraman 2000, Mason and Graham 2002).

4 Empirical examples

We return to the empirical ROC curves in Figure 2 and present basic information about the underlying datasets in Table 3. In the dataset from Etzioni et al. (1999), the negative logarithm of the ratio of free to total prostate-specific antigen (PSA) two years prior to diagnosis in serum from patients later found to have prostate cancer is compared to age-matched controls. The datasets from Sing et al. (2005, Figure 1a) and Robin et al. (2011, Figure 1) are prominent examples in the widely used `ROCR` and `pROC` packages in R. They concern a score from a linear support vector machine (SVM) trained to predict the usage of HIV coreceptors, and the S100 β biomarker as it relates to a binary clinical outcome, respectively. The dataset from Vogel et al. (2018, Figure 6d) considers probability of precipitation forecasts from the European Centre for Medium-Range Weather Forecasts (ECMWF) numerical weather prediction (NWP) ensemble system (Molteni et al. 1996) for the binary event of precipitation occurrence within the next 24 hours at meteorological stations in the West Sahel region in northern tropical Africa.

Figure 7 shows binormal and beta ROC curves fitted to the empirical ROC curves, both in the unrestricted case and under the constraint of concavity. The respective unrestricted and restricted minimum distance estimates, the fit in terms of the L_2 -distance to the empirical ROC curve, and the p -value from the goodness-of-fit test in Section 3.3

Table 3: Basic information about the datasets and minimum distance estimates under the unrestricted and concave binormal and beta models for the ROC curves in Figures 2 and 7. Fit is in terms of the L_2 -distance to the empirical ROC curve, and the p -value is from the goodness-of-fit test of Section 3.3.

Dataset	Etzioni et al. (1999)	Sing et al. (2005)	Robin et al. (2011)	Vogel et al. (2018)
Binary outcome	prostate cancer	coreceptor usage	clinical outcome	precipitation
Feature	antigen ratio	SVM predictor	S100 β concentr.	NWP forecast
Sample size	116	3450	113	5449
Binormal model				
unrestricted (μ, σ)	(1.05, 0.78)	(1.58, 0.65)	(0.75, 0.72)	(1.13, 1.22)
fit	0.043	0.019	0.033	0.008
p -value	0.106	0.001	0.561	0.032
concave (μ, σ)	(1.22, 1.00)	(2.05, 1.00)	(0.91, 1.00)	(0.99, 1.00)
fit	0.056	0.039	0.060	0.031
p -value	0.138	0.001	0.147	0.001
Beta model				
unrestricted (α, β)	(0.34, 1.32)	(0.15, 1.44)	(0.36, 0.96)	(0.79, 2.57)
fit	0.042	0.023	0.032	0.006
p -value	0.117	0.001	0.620	0.187
concave (α, β)	(0.38, 1.62)	(0.17, 1.83)	(0.51, 1.49)	(0.79, 2.57)
fit	0.045	0.025	0.050	0.006
p -value	0.196	0.001	0.204	0.171

with $M = 999$ Monte Carlo replicates, are given in Table 3. In the unrestricted case, the binormal and beta fits are visually nearly indistinguishable. The fitted binormal ROC curves fail to be concave and change markedly when concavity is enforced. For the beta ROC curves, the differences between restricted and unrestricted fits are less pronounced, and in the example from Vogel et al. (2018) the unrestricted fit is concave. Generally, in the constrained case the improvement in the fit under the more flexible beta model as compared to the classical binormal model is substantial.

The theoretical results in Section 3.2 allow for asymptotic inference about the model parameters. We illustrate this in Figure 8 for the unrestricted beta fit for the dataset from Etzioni et al. (1999). In addition to showing confidence ellipsoids, we indicate and separate concave and non-concave fits. If we seek to complement the minimum distance estimate with pointwise confidence bands for the ROC curve, we can sample from the inferred distribution for the model parameters and display the envelope of the respective ROC curves, as exemplified in Figure 10 below.

A closer look at the empirical ROC curves for the biomedical data from Etzioni et al. (1999), Sing et al. (2005) and Robin et al. (2011) in Figures 2 and 7 reveals a striking commonality, in that the curves show vertical and/or horizontal straight edges. From the definition of the raw ROC characteristic (2) it is evident that vertical straight edges correspond to marker values that may allow for deterministic class attribution, as illustrated in the back-to-back histograms in Figure 9. Importantly, straight edges

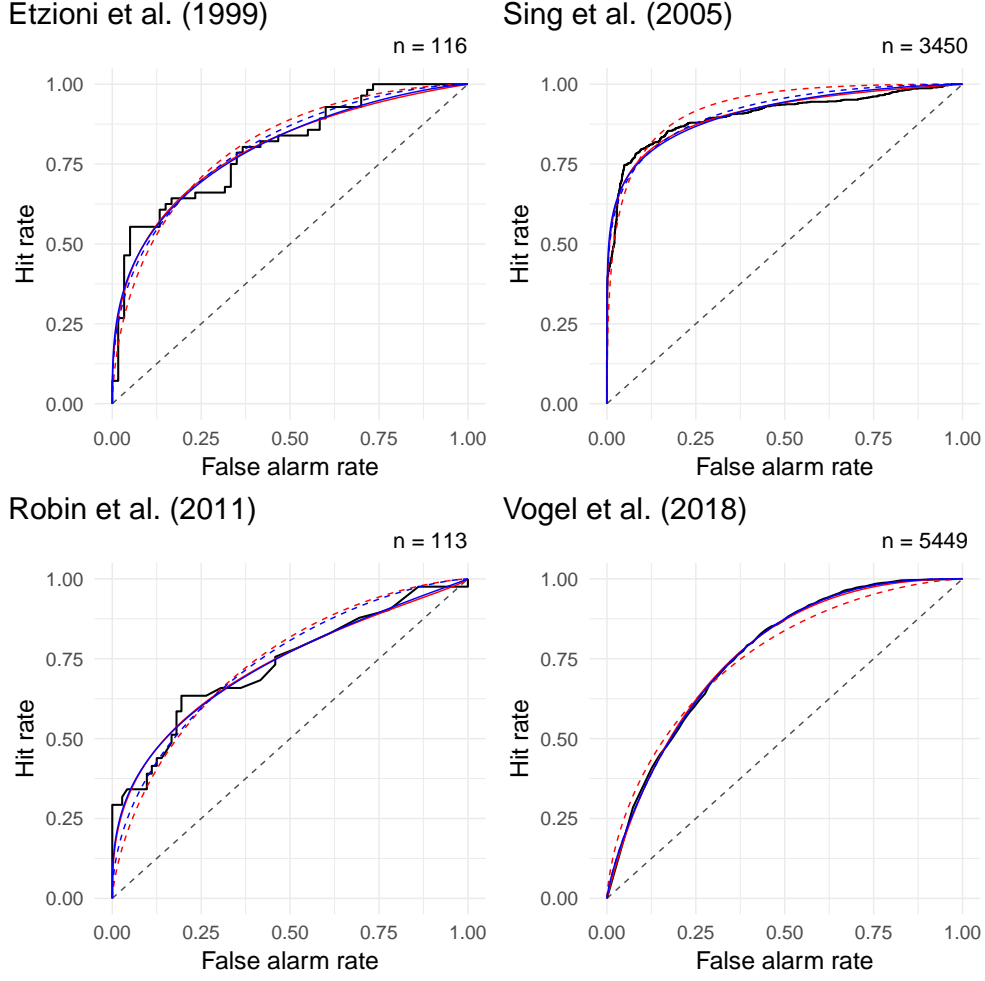


Figure 7: Fitted binormal (red) and beta (blue) ROC curves in the unrestricted (solid) and concave (dashed) case for the datasets from Figure 2 and Table 3.

might convey critical information from a subject matter perspective, such as in medical diagnoses, where straight edges in ROC curves correspond to particularly high or low marker values that might identify individuals as healthy or diseased beyond doubt.

Under the beta family the statistical modeling of straight edges is straightforward. Specifically, we can generalize the two-parameter model (6) to a four-parameter beta family, where

$$R(p) = \gamma + (1 - \gamma) B_{\alpha, \beta} \left(\frac{p}{\delta} \right) \quad \text{for } p \in (0, 1], \quad (12)$$

which allows for a vertical straight edge that connects the coordinate origin $(0, 0)'$ to the point $(0, \gamma)'$, and a horizontal straight edge that connects the points $(\delta, 1)'$ and $(1, 1)'$ within the ROC curve. Three-parameter subfamilies with a single type of straight edge arise if we fix $\delta = 1$ and let $\gamma \in [0, 1]$ vary, or fix $\gamma = 0$ and consider $\delta \in (0, 1]$,

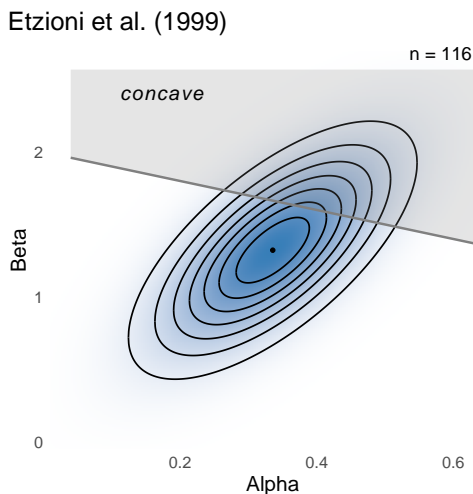


Figure 8: Asymptotic inference under the unrestricted beta model for the data from Etzioni et al. (1999). The confidence ellipses are at level $1/8, 2/8, \dots, 7/8$, respectively.

respectively. While the subfamily with $\delta = 1$ being fixed has a direct analogue under the binormal model, there is no natural way of adapting the subfamily with $\gamma = 0$ being fixed or the four-parameter family in (12) to the binormal case.

To be clear, we do *not* advocate uncritical routine use of the four-parameter family in (12) and the respective three-parameter subfamilies. However, we *do* recommend that in any specific application researchers check for straight edges in empirical ROC curves, and assess on the basis of substantive expertise whether or not they ought to be modeled. Visual tools such as the back-to-back histograms for the conditional distributions in Figure 9 can assist in this assessment. For illustration, the back-to-back histograms might suggest that we fit the three-parameter model with $\gamma = 0$ being fixed to the data from Etzioni et al. (1999) and the three-parameter model with $\delta = 1$ being fixed to the data from Sing et al. (2005) and Robin et al. (2011). While in the first two cases the three-parameter fits are nearly identical to the fits under the two-parameter beta model, the three-parameter extension yields a substantially improved fit for the data from Robin et al. (2011), as illustrated in the lower right panel of Figure 9. The constrained minimum distance estimate for (α, β, γ) is $(0.70, 1.30, 0.24)$ with L_2 -distance 0.029 to the empirical ROC curve. For comparison, under the two-parameter concave beta model the estimate for (α, β) is $(0.51, 1.49)$ with L_2 -distance 0.050.

Finally, we take another look at the meteorological data from Vogel et al. (2018). Here it is obvious from the scientific context in weather prediction that the above three- and four-parameter extensions are irrelevant. While the data introduced and analyzed in Table 3 and Figures 2 and 7 concern probability of precipitation forecasts over the West Sahel region, Vogel et al. (2018) consider the East Sahel region as well. The respective empirical ROC curves are shown in Figure 10 along with the constrained two-parameter beta fit and parametric 95% pointwise confidence bands. The p -value for the

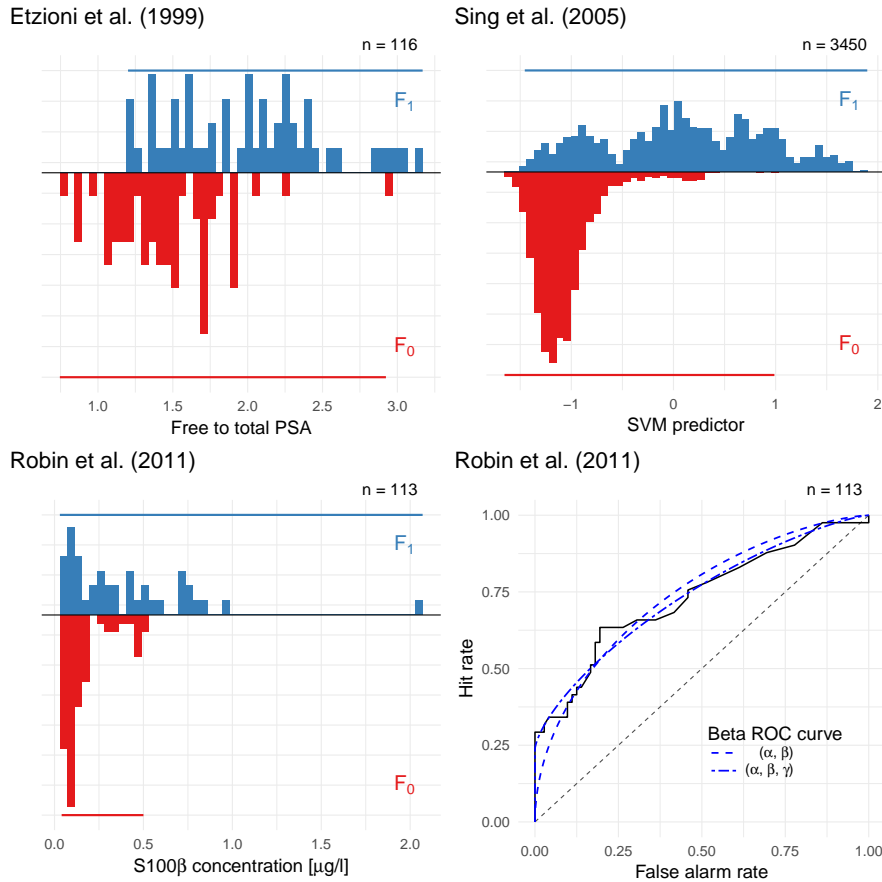


Figure 9: Histograms for the conditional distributions for data in Table 3, and concave two- and three-parameter beta ROC curves fit to the data from Robin et al. (2011). The horizontal lines in the histograms extend to the convex hull of the respective support.

goodness-of-fit test of Section 3.3 is 0.168 for West Sahel and 0.057 for East Sahel. Our parametric tests for equality of AUC values and ROC curves yield p -values of 0.633 and 0.015, whereas the nonparametric tests of DeLong et al. (1988) and Venkatraman (2000) result in p -values of 0.616 and 0.089, respectively.

5 Discussion

ROC curves have been used extensively to evaluate the potential predictive value of covariates, features, or markers in binary problems in a multitude of scientific disciplines. Their appeal stems from attractive and desirable properties in this context, which include the straightforward interpretation of ROC curves in terms of attainable operating conditions (i.e., hit and false alarm rates), their invariance under strictly increasing transformations of the feature and shifts in prevalence, and the interpretation of AUC

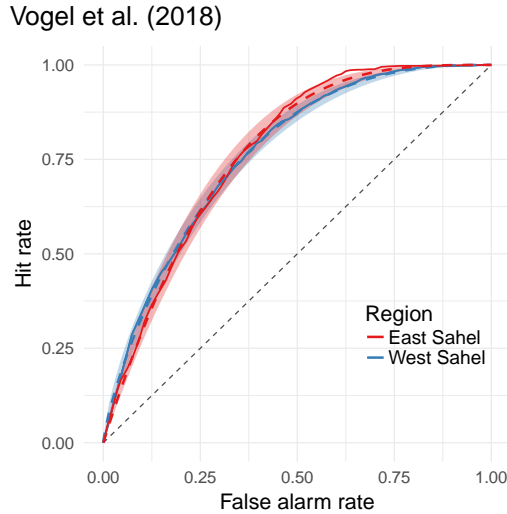


Figure 10: Empirical ROC curve (solid), concave beta fit (dashed), and associated point-wise 95% confidence band for data from Vogel et al. (2018) on probability of precipitation forecasts over West and East Sahel in northern tropical Africa.

as the probability of a marker value drawn from F_1 being higher than a value drawn independently from F_0 . We emphasize that ROC curves and AUC values “should be regarded as a measure of potential rather than actual skill” (Kharin and Zwiers 2003, p. 4148) tailored to serve the purposes of variable selection and feature screening across all types of ordinal, discrete, and continuous predictor variables.⁴

Despite their ubiquitous use, our understanding of fundamental properties of ROC curves has been incomplete. The theoretical results in Section 2 establish an equivalence between ROC curves and the CDFs of probability measures on the unit interval, which motivates and justifies our curve fitting approach to the modelling of ROC curves. Concave fits are preferred, if not essential, as they characterize the predictor variables with nondecreasing likelihood ratios and nondecreasing conditional event probabilities. The beta family (6) provides a particularly attractive parametric model. As compared to the classical binormal model the beta family is considerably more flexible under the constraint of concavity, and it embeds naturally into the four-parameter model (12) that allows for straight edges in the ROC curve. If further flexibility is sought, mixtures of beta CDFs can be fitted. With a view toward nonparametric alternatives, one might model (minus) the second derivative of a regular ROC curve, which is nonnegative under the concavity constraint.

⁴ROC curves and AUC values have limitations when they are used to assess the actual skill of probability forecasts, as they ignore the critical requirement of calibration (Wilks 2011, p. 346). For evaluating the *actual* skill and value of probabilistic classifiers, proper scoring rules (Gneiting and Raftery 2007) are a preferred tool, notably in the form of Murphy diagrams (Ehm et al. 2016). For a direct comparison of ROC curves and Murphy diagrams and a respective discussion in the context of probability forecasts see Figure 6 and Sections 2.c and 4 of Vogel et al. (2018).

For estimation we focus on the minimum distance approach. In the regular setting, where features are continuous, minimum distance estimates and associated parametric estimates of the AUC value are asymptotically normal. Goodness of fit and other hypotheses can be tested for based on these methods and results. In view of the critical role of concavity for the interpretation of ROC curves, an interesting and relevant question is whether or not one should subject features to the PAV algorithm (de Leeuw et al. 2009) prior to fitting a concave model. The PAV algorithm morphs the empirical ROC curve into the respective concave hull, and its use for data pre-processing in other types of shape-constrained estimation problems has been examined by Mammen (1991). The derivation of the large sample distributions in Section 3.2 is based on empirical process theory (Shorack and Wellner 2009), and it depends on the Gaussian limit in (7), which does not apply under ordinal or discrete features nor when ROC curves have straight edges. We leave the derivation of large sample distributions for minimum distance estimates in these cases as well as adaptations to covariate- and time-dependent settings (Etzioni et al. 1999, Heagerty et al. 2000) to future work.

Datasets and code in R (R Core Team 2017) for replicating our results and implementing the proposed estimators and tests is available from Peter Vogel. We are working towards an R package tentatively named `betaROC`, to be released shortly.

Acknowledgments

The research leading to these results has been accomplished within project C2 “Prediction of wet and dry periods of the West African monsoon” of the Transregional Collaborative Research Center SFB / TRR 165 “Waves to Weather” funded by the German Science Foundation (DFG). Tilmann Gneiting thanks the Klaus Tschira Foundation for generous support, and we are grateful to Alexander Jordan, Johannes Resin, and our meteorological collaborators Andreas H. Fink, Peter Knippertz, and Andreas Schlueter for a wealth of comments and continuous encouragement.

A Appendix: Proofs

A.1 Concave ROC curves: The discrete setting

In proving Theorem 4 we may assume that the support of X is a finite or countably infinite, ordered set of two or more points x_i , indexed by consecutive integers such that $x_i < x_j$ if $i < j$. In the case of a finite set we assume that it is of cardinality at least 2 and adapt the arguments in obvious ways to account for boundary effects.

Lemma 12. *Any of the statements in Theorem 4 implies that either*

- (i) $\mathbb{Q}(X = x_i | Y = 0) > 0$ for all i , or
- (ii) there exists an index value i^* such that $\mathbb{Q}(X = x_i | Y = 0) = 0$ for all $i \geq i^*$ and $\mathbb{Q}(X = x_i | Y = 0) > 0$ for all $i < i^*$.

Proof. If any of the statements in Theorem 4 hold and condition (i) is violated, there exists an index i such that $\mathbb{Q}(X = x_i | Y = 0) = 0$. Then $\text{CEP}(x_i) = 1$, $\text{LR}(x_i) = \infty$, and the ROC curve

has a vertical straight edge, which contradicts statements (c), (b), and (a), respectively, unless condition (ii) is satisfied and the straight edge is at the origin. \square

Proof of Theorem 4. In view of Lemma 12, it suffices to show the equivalence of the statements in Theorem 4 for indices i with $\mathbb{Q}(X = x_i | Y = 0) > 0$. The fact that

$$\text{LR}(x_i) = \frac{\pi_0}{\pi_1} \frac{\text{CEP}(x_i)}{1 - \text{CEP}(x_i)}$$

along with the monotonicity of the function $c \mapsto c/(1 - c)$ establishes the equivalence of (b) and (c). Furthermore, the relationship

$$\begin{aligned} \text{LR}(x_i) &= \frac{\mathbb{Q}(X = x_i | Y = 1)}{\mathbb{Q}(X = x_i | Y = 0)} \\ &= \frac{\mathbb{Q}(X > x_{i-1} | Y = 1) - \mathbb{Q}(X > x_i | Y = 1)}{\mathbb{Q}(X > x_{i-1} | Y = 0) - \mathbb{Q}(X > x_i | Y = 0)} \\ &= \frac{\text{HR}(x_{i-1}) - \text{HR}(x_i)}{\text{FAR}(x_{i-1}) - \text{FAR}(x_i)} \end{aligned}$$

implies that

$$\text{LR}(x_{i+1}) \geq \text{LR}(x_i) \Leftrightarrow \frac{\text{HR}(x_i) - \text{HR}(x_{i+1})}{\text{FAR}(x_i) - \text{FAR}(x_{i+1})} \geq \frac{\text{HR}(x_{i-1}) - \text{HR}(x_i)}{\text{FAR}(x_{i-1}) - \text{FAR}(x_i)}$$

and the right-hand side is equivalent to the ROC curve being concave, thereby demonstrating the equivalence of (a) and (b). \square

A.2 Properties of beta ROC curves

Lemma 13. *The AUC value for the beta ROC curve is $\beta/(\alpha + \beta)$.*

Proof. We have

$$\text{AUC}(\alpha, \beta) = \int_0^1 B_{\alpha, \beta}(p) \, dp = \left[p B_{\alpha, \beta}(p) - \frac{\alpha}{\alpha + \beta} B_{\alpha+1, \beta}(p) \right]_0^1 = 1 - \frac{\alpha}{\alpha + \beta},$$

as claimed. \square

Lemma 14. *The CDF of the beta distribution is concave if and only if $\alpha \leq 1$ and $\beta \geq 2 - \alpha$, and it is strictly concave if furthermore $\alpha < 1$.*

Proof. The density $b_{\alpha, \beta}$ of the beta distribution satisfies

$$b'_{\alpha, \beta}(x) = \frac{\alpha - 1 + (2 - \alpha - \beta)x}{x(1 - x)} b_{\alpha, \beta}(x)$$

for $x \in (0, 1)$, from which the statement is immediate. \square

Proof of Theorem 9. We apply the natural identification and define F_{NI} as in (4). Due to the assumption of strong regularity, F_{NI} admits a density on $(0, 1)$ that can be extended to a continuous function f_{NI} on $[0, 1]$. The arguments in Bernstein's probabilistic proof of the Weierstrass approximation theorem (Levasseur 1984) show that as $n \rightarrow \infty$ the sequence

$$m_n(q) = \frac{1}{n+1} \sum_{k=0}^n f_{\text{NI}}\left(\frac{k}{n}\right) b_{k+1, n-k+1}(q)$$

converges to $f_{\text{NI}}(q)$ uniformly in $q \in [0, 1]$. Furthermore,

$$a_n = \int_0^1 m_n(q) \, dq \rightarrow \int_0^1 f_{\text{NI}}(q) \, dq = 1$$

as $n \rightarrow \infty$, and for $n = 1, 2, \dots$ the mapping $p \mapsto M_n(p) = \int_0^p m_n(q) \, dq / a_n$ represents a mixture of beta CDFs. The uniform convergence of m_n to f_{NI} implies that for every $\epsilon > 0$ there exists an n' such that

$$\begin{aligned} |F_{\text{NI}}(p) - M_n(p)| &\leq \int_0^p \left| f_{\text{NI}}(q) - \frac{m_n(q)}{a_n} \right| \, dq \\ &\leq \int_0^p \left| f_{\text{NI}}(q) - \frac{f_{\text{NI}}(q)}{a_n} \right| \, dq + \frac{1}{a_n} \int_0^p |f_{\text{NI}}(q) - m_n(q)| \, dq \\ &\leq \left| 1 - \frac{1}{a_n} \right| + \frac{1}{a_n} \int_0^p |f_{\text{NI}}(q) - m_n(q)| \, dq < \epsilon \end{aligned}$$

for all integers $n > n'$ uniformly in $p \in [0, 1]$. The statement of the theorem follows. \square

A.3 Asymptotic normality of minimum distance estimates

Here we demonstrate the asymptotic normality of the minimum distance estimator $\hat{\theta}_n$ in the setting of Section 3.2. In a nutshell, we apply Theorem 2.2 of Hsieh and Turnbull (1996) and Theorem 3.6 along with the results in Section II in the fundamental paper on minimum distance estimation by Millar (1984). In contrast to the results in Section 4 of Hsieh and Turnbull (1996), which concern minimum distance estimation for the binormal model and ordinal dominance curves, Theorem 10 applies to general parametric families and ROC curves.

Proof of Theorem 10. We are in the setting of Theorem 2.2 of Hsieh and Turnbull (1996), according to which there exists a probability space with sequences $(B_{1,n})$ and $(B_{2,n})$ of independent versions of Brownian bridges such that

$$\sqrt{n} \xi_n(p; \theta_0) = \sqrt{\lambda} B_{1,n}(R(p; \theta_0)) + R'(p; \theta_0) B_{2,n}(p) + o\left(n^{-1/2}(\log n)^2\right) \quad (13)$$

almost surely, and uniformly in p on every interval $[a, b] \subset (0, 1)$. We proceed to verify the regularity conditions for Theorem 3.6 of Millar (1984). As regards the identifiability condition (3.2) and the differentiability condition (3.5) it suffices to note that

$$\xi_n(p; \theta) - \xi_n(p; \theta_0) = R(p; \theta) - R(p; \theta_0)$$

is nonrandom, continuously differentiable with respect to p and the components of the parameter vector θ , and independent of n . The boundedness condition (3.3) is trivially satisfied and the convergence condition (3.4) is implied by (13). Finally, we apply⁵ (2.17), (2.18), (2.19), and (2.20) in Section II of Millar (1984) to yield (8) and (9), where the covariance function of the process in (7) is

$$\begin{aligned} K(s, t; \theta) &= \text{Cov}(W(s; \theta), W(t; \theta)) \\ &= \lambda \text{Cov}(B_1(R(s; \theta)), B_1(R(t; \theta))) + R'(s; \theta) R'(t; \theta) \text{Cov}(B_2(s), B_2(t)) \\ &= \lambda (\min\{R(s; \theta), R(t; \theta)\} - R(s; \theta) R(t; \theta)) + R'(s; \theta) R'(t; \theta) (\min\{s, t\} - st), \end{aligned}$$

whence $K(s, t; \theta_0)$ is as stated in (10). \square

⁵We note a typographical error in eq. (2.20) of Millar (1984), where the asymptotic covariance matrix is incorrectly specified as $C^{-1}AC$; it should read $C^{-1}AC^{-1}$ instead.

The asymptotic result in Corollary 11 follows in a straightforward application of the delta method.

References

- Ayer, M., Brunk, H., Ewing, G., Reid, W. and Silverman, E. (1955). An empirical distribution function for sampling with incomplete information. *Annals of Mathematical Statistics*, **5**, 641–647.
- Bradley, A. P. (1997). The use of the area under the ROC curve in the evaluation of machine learning algorithms. *Pattern Recognition*, **30**, 1145–1159.
- DeLong, E. R., DeLong, D. and Clarke-Pearson, D. L. (1988). Comparing the areas under two or more correlated receiver operating characteristic curves: A nonparametric approach. *Biometrics*, **44**, 837–845.
- Dorfman, D. D. and Alf, E. (1969). Maximum-likelihood estimation of parameters of signal-detection theory and determination of confidence intervals — rating-method data. *Journal of Mathematical Psychology*, **6**, 487–496.
- Egan, J. P. (1975). *Signal Detection Theory and ROC Analysis*. Academic Press, New York.
- Egan, J. P., Greenberg, G. Z. and Schulman, A. I. (1961). Operating characteristics, signal detectability, and the method of free response. *Journal of the Acoustical Society of America*, **33**, 993–1007.
- Ehm, W., Gneiting, T., Jordan, A. and Krüger, F. (2016). Of quantiles and expectiles: Consistent scoring functions, Choquet representations and forecast rankings (with discussion and rejoinder). *Journal of the Royal Statistical Society Series B: Statistical Methodology*, **78**, 505–562.
- Etzioni, R., Pepe, M., Longton, G., Hu, C. and Goodman, G. (1999). Incorporating the time dimension in receiver operating characteristic curves: A case study of prostate cancer. *Medical Decision Making*, **19**, 242–251.
- Fawcett, T. (2006). An introduction to ROC analysis. *Pattern Recognition Letters*, **27**, 861–874.
- Fawcett, T. and Niculescu-Mizil, A. (2007). PAV and the ROC convex hull. *Machine Learning*, **68**, 97–106.
- Gneiting, T. and Raftery, A. E. (2007). Strictly proper scoring rules, prediction, and estimation. *Journal of the American Statistical Association*, **102**, 359–378.
- Hanley, J. A. and McNeil, B. J. (1982). The meaning and use of the area under a receiver operating characteristic (ROC) curve. *Radiology*, **143**, 29–36.
- Hanley, J. A. and McNeil, B. J. (1983). A method of comparing the areas under receiver operating characteristic curves derived from the same cases. *Radiology*, **148**, 839–843.
- Heagerty, P. J., Lumley, T. and Pepe, M. S. (2000). Time-dependent ROC curves for

- censored survival data and a diagnostic marker. *Biometrics*, **56**, 337–344.
- Hilden, J. (1991). The area under the ROC curve and its competitors. *Medical Decision Making*, **11**, 95–101.
- Hsieh, F. and Turnbull, B. W. (1996). Nonparametric and semiparametric estimation of the receiver operating characteristic curve. *Annals of Statistics*, **24**, 25–40.
- Kharin, V. V. and Zwiers, F. (2003). On the ROC score of probability forecasts. *Journal of Climate*, **16**, 4145–4150.
- Krzanowski, W. J. and Hand, D. J. (2009). *ROC Curves for Continuous Data*. CRC Press, Boca Raton.
- de Leeuw, J., Hornik, K. and Mair, P. (2009). Isotone optimization in R: Pool-Adjacent-Violators Algorithm (PAVA) and active set methods. *Journal of Statistical Software*, **32** (5), 1–24.
- Levasseur, K. M. (1984). A probabilistic proof of the Weierstrass approximation theorem. *American Mathematical Monthly*, **91**, 249–250.
- Lloyd, C. J. (2002). Estimation of a convex ROC curve. *Statistics & Probability Letters*, **59**, 99–111.
- Mammen, E. (1991). Estimating a smooth monotone regression function. *Annals of Statistics*, **19**, 724–740.
- Mason, S. J. and Graham, N. E. (2002). Areas beneath the relative operating characteristic (ROC) and relative operating levels (ROL) curves: Statistical significance and interpretation. *Quarterly Journal of the Royal Meteorological Society*, **128**, 2145–2166.
- Metz, C. E. and Kronman, H. B. (1980). Statistical significance tests for binormal ROC curves. *Journal of Mathematical Psychology*, **22**, 218–243.
- Metz, C. E., Herman, B. A. and Shen, J.-H. (1998). Maximum likelihood estimation of receiver operating characteristic (ROC) curves from continuously-distributed data. *Statistics in Medicine*, **17**, 1033–1053.
- Millar, P. W. (1984). A general approach to the optimality of minimum distance estimators. *Transactions of the American Mathematical Society*, **286**, 377–418.
- Molteni, F., Buizza, R., Palmer, T. N. and Petroliagis, T. (1996). The ECMWF ensemble prediction system: Methodology and validation. *Quarterly Journal of the Royal Meteorological Society*, **122**, 73–119.
- Nelsen, R. B. (2006). *An Introduction to Copulas*, second edition. Springer, New York.
- Pepe, M. S. (2000). An interpretation for the ROC curve and inference using GLM procedures. *Biometrics*, **56**, 352–359.
- Pepe, M. S. (2003). *The Statistical Evaluation of Medical Tests for Classification and Prediction*. Oxford University Press, Oxford.
- Pesce, L. L., Metz, C. E. and Berbaum, K. S. (2010). On the convexity of ROC curves estimated from radiological results. *Academic Radiology*, **17**, 960–968.

- R Core Team (2017). R: A language and environment for statistical computing. R Foundation for Statistical Computing, Vienna, Austria, <http://www.R-project.org/>.
- Robin, X., Turck, N., Hainard, A., Tiberti, N., Lisacek, F., Sanchez, J.-C. and Müller, M. (2011). pROC: An open-source package for R and S+ to analyze and compare ROC curves. *BMC Bioinformatics*, **12**, 77.
- Shorack, G. R. and Wellner, J. A. (2009). *Empirical Processes with Applications to Statistics*. SIAM, Philadelphia.
- Sing, T., Sander, O., Beerenwinkel, N. and Lengauer, T. (2005). ROCR: Visualizing classifier performance in R. *Bioinformatics*, **21**, 3940–3941.
- Swets, J. A. (1973). The relative operating characteristic in psychology. *Science*, **182**, 990–1000.
- Swets, J. A. (1986). Indices of discrimination or diagnostic accuracy. *Psychological Bulletin*, **99**, 100–117.
- Swets, J. A. (1988). Measuring the accuracy of diagnostic systems. *Science*, **240**, 1285–1293.
- Venkatraman, E. S. (2000). A permutation test to compare receiver operating characteristic curves. *Biometrics*, **56**, 1134–1138.
- Venkatraman, E. S. and Begg, C. B. (1996). A distribution-free procedure for comparing receiver operating characteristic curves from a paired experiment. *Biometrika*, **83**, 835–848.
- Vogel, P., Knippertz, P., Fink, A. H., Schlueter, A. and Gneiting, T. (2018). Skill of global raw and postprocessed ensemble predictions of rainfall over northern tropical Africa. *Weather and Forecasting*, **33**, 369–388.
- Wilks, D. S. (2011). *Statistical Methods in the Atmospheric Sciences*, third edition. Elsevier Academic Press, Amsterdam.
- Zhou, X.-H., Obuchowski, N. A. and McClish, D. K. (2011). *Statistical Methods in Diagnostic Medicine*, second edition. Wiley, Hoboken.
- Zou, K. H. and Hall, W. J. (2000). Two transformation models for estimating an ROC curve derived from continuous data. *Journal of Applied Statistics*, **27**, 621–631.
- Zou, K. H., Resnic, F. S., Talos, I.-F., Goldberg-Zimring, D., Bhagwat, J. G., Haker, S. J., Kikinis, R., Jolesz, F. A. and Ohno-Machado, L. (2005). A global goodness-of-fit test for receiver operating characteristic curve analysis via the bootstrap method. *Journal of Biomedical Informatics*, **38**, 395–403.
- Zweig, M. H. and Campbell, G. (1993). Receiver-operating characteristic (ROC) plots: A fundamental evaluation tool in clinical medicine. *Clinical Chemistry*, **39**, 561–577.